AD-A187 224 PULSED CURRENT TRANSFORMER FOR LOW INDUCTIVE LOADS(U) 1/1
ARMY BALLISTIC RESEARCH LAB ABERDEEN PROVING GROUND MD
A ZIELINSKI ET AL. OCT 87 BRL-MR-3626

UNCLASSIFIED F/G 10/2 NL

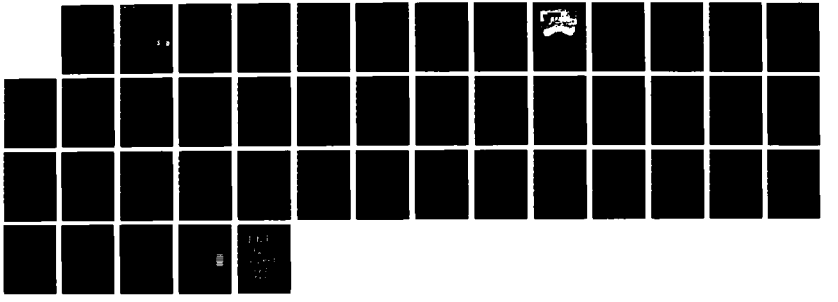

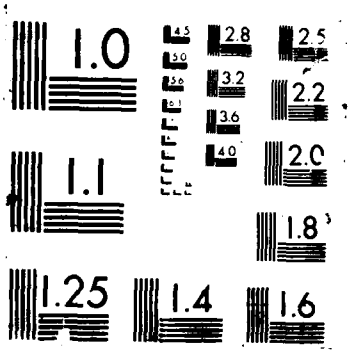
1.0
1.1
1.25
1.4
1.6
1.8
2.0
2.2
2.5
2.8
3.2
3.6
4.0
4.5
5.0
5.6

AD

(2)

MEMORANDUM REPORT BRL-MR-3626

PULSED CURRENT TRANSFORMER FOR LOW INDUCTIVE LOADS

ALEX ZIELINSKI
KEITH JAMISON
JOHN BENNETT

OCTOBER 1987

US ARMY BALLISTIC RESEARCH LABORATORY
ABERDEEN PROVING GROUND, MARYLAND

UNCLASSIFIED

SECURITY CLASSIFICATION OF THIS PAGE

REPORT DOCUMENTATION PAGE

Form Approved
OMB No 0704 0188
Exp Date Jun 30 1986

1a REPORT SECURITY CLASSIFICATION UNCLASSIFIED	1b RESTRICTIVE MARKINGS
2a SECURITY CLASSIFICATION AUTHORITY	3 DISTRIBUTION / AVAILABILITY OF REPORT
2b DECLASSIFICATION / DOWNGRADING SCHEDULE	
4 PERFORMING ORGANIZATION REPORT NUMBER(S) BRL-MR-3626	5 MONITORING ORGANIZATION REPORT NUMBER(S)
6a NAME OF PERFORMING ORGANIZATION US Army Ballistic Research Laboratory 6b OFFICE SYMBOL (If applicable) SLCBR-TB-EP	7a NAME OF MONITORING ORGANIZATION
6c ADDRESS (City, State, and ZIP Code) Aberdeen Proving Ground, MD 21005-5066	7b ADDRESS (City, State, and ZIP Code)
8a NAME OF FUNDING / SPONSORING ORGANIZATION US Army Ballistic Research Laboratory 8b OFFICE SYMBOL (If applicable) SLCBR-D	9 PROCUREMENT INSTRUMENT IDENTIFICATION NUMBER
8c ADDRESS (City, State, and ZIP Code) Aberdeen Proving Ground, MD 21005-5066	10 SOURCE OF FUNDING NUMBERS PROGRAM ELEMENT NO: 62618A; PROJECT NO: AH80; TASK NO: 00; WORK UNIT ACCESSION NO: 001AJ

11 TITLE (Include Security Classification)

(U) Pulsed Current Transformer for Low Inductance Loads

12 PERSONAL AUTHOR(S)

Zielinski, Alexander, Jamison, Keith (BRL) and Bennett, John (ARDEC)

13a TYPE OF REPORT	13b TIME COVERED FROM _____ TO _____	14 DATE OF REPORT (Year, Month, Day)	15 PAGE COUNT

16 SUPPLEMENTARY NOTATION

17 COSATI CODES			18 SUBJECT TERMS (Continue on reverse if necessary and identify by block number)
FIELD	GROUP	SUB-GROUP	Electromagnetic Railgun, Pulse Transformer, Pulse Power, High Current Transformer
10	01		
21	03		

19 ABSTRACT (Continue on reverse if necessary and identify by block number) (idk)

At the US Army Research, Development and Engineering Command (ARDEC), an effort was undertaken to couple an array of five capacitor banks to a low inductance load. To achieve currents which exceed the limit placed on the capacitor banks, pulse current transformers were used. This power system, termed CAPSTAR, was ultimately used to electromagnetically stress a round bore composite railgun barrel section.

A mathematical model has been developed to simulate a capacitor power supply driving a pulse transformer with various secondary loads. The model was first tested by comparison to experimental results using a subscale pulse transformer. The calculated data points were in good agreement with the experiment. Minor adjustments to some circuit parameters to account for the transitory behavior of the circuit are described.

The ARDEC system of five capacitor banks and pulse transformers was evaluated in the same way as the subscale transformer. Measurements for evaluating the (Continued)

20 DISTRIBUTION / AVAILABILITY OF ABSTRACT	21 ABSTRACT SECURITY CLASSIFICATION	
☒ UNCLASSIFIED-UNLIMITED ☐ SAME AS RPT ☐ DTIC USERS	UNCLASSIFIED	
22a NAME OF RESPONSIBLE INDIVIDUAL Alexander Zielinski	22b TELEPHONE (Include Area Code) (301) 278-3889	22c OFFICE SYMBOL SLCBR-TB-EP

DD FORM 1473, 84 MAR

83 APR edition may be used until exhausted
All other editions are obsolete

SECURITY CLASSIFICATION OF THIS PAGE

UNCLASSIFIED

19. [illegible] were made on only one of the five capacitor banks and it was assumed that the remaining four were identical to the first. Possibly because of this assumption, the agreement between model and experiment was not as close as with the subscale transformer. Performance curves allowing load optimization for the CAPSTAR system are presented.

In the performance simulations, not only were constant inductive and resistive loads used, but a railgun was also modeled as a load. Performance has been plotted for two power sources; the five capacitor banks in parallel with a pulse shaping inductor and the CAPSTAR system. In all cases the capacitor banks were crowbarred. The pulse transformers perform best when driving a short, large-bore railgun.

ACKNOWLEDGEMENT

The authors wish to thank the personnel at ARDEC (Army Research, Development and Engineering Command) for supplying the test data on the CAPSTAR system.

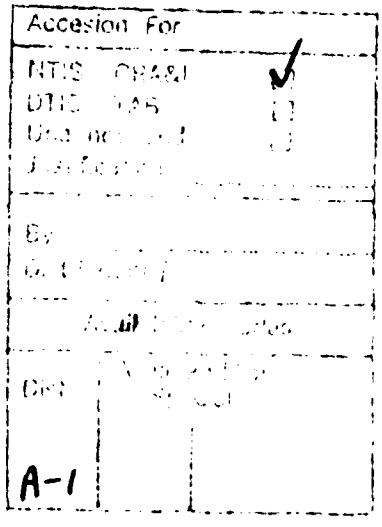

TABLE OF CONTENTS

LIST OF ILLUSTRATIONS

I. INTRODUCTION

The concept of accelerating particles using an electromagnetic railgun has been pursued for many years. Railguns and their subcomponents are low impedance devices which require a power source capable of producing high currents. There are a limited number of sources which can meet these requirements. Among these are rotating machines, which often need constant, careful maintenance and, typically, create a pulse with a long risetime. Capacitors are also able to supply large currents. They are readily available and relatively maintenance free. They must, however, be used with a pulse forming network to protect them from discharging too quickly. This protection is usually in the form of an internal impedance which limits the minimum discharge time and the peak current delivered from the power source.

The ARDEC Electromagnetic Launcher Facility, Picatinny Arsenal, Dover, NJ, has five, 50 kilojoule, 10,000 volt, capacitor banks each having a maximum current rating of 100,000 amperes. This current limit must be observed to prevent internal damage to the supply. It also makes tnese banks unsuitable for pulsing loads which have an inductance less than one microhenry. One method to alleviate this, and achieve protection, is to operate the capacitor bank in conjunction with a pulse transformer. Five coaxial pulse transformers were designed and built at the University of Texas, Center for Electromechanics, Austin, TX.[1] The ultimate goal of this project was to operate all five pulse transformers, each driven by a capacitor bank, in parallel, to deliver a current pulse of two million amperes to a short section of a composite railgun barrel. The integrated system of capacitor banks and current step-up pulse transformers has been named CAPSTAR. The laboratory set-up of the system is shown in the top of Fig. 1. As a means for validating CAPSTAR, a single, subscale pulse transformer was constructed to verify estimates of performance and to corroborate the mathematical model.

The purpose of this paper is to describe the mathematical model we have developed, report the verification done with the subscale pulse transformer and CAPSTAR, and present the results from the initial testing of the CAPSTAR system. In Sec. II of this report, we present an equivalent circuit for the pulse transformer driving an arbitrary load and outline the method we have used to solve the equations. In Sec. III, the physical behavior of the pulse transformer is discussed. In Secs. IV and V, we show both calculated and measured electrical properties for each of the components in the transformer system. Section VI describes a simulation of the performance of both the subscale and CAPSTAR systems and the last section discusses the output from the simulation and expected performance if the CAPSTAR system were used to drive a railgun armature.

II. CIRCUIT MODEL

Consider the equivalent circuit representation for a capacitor driving the primary of a current step up pulse transformer as shown in the lower portion of Fig. 1. The secondary winding of the transformer is connected to a

[1]Pappas, J.A., Driga, M.D. and Weldon, W.F., "High Current Coaxial Pulse Transformer for Railgun Applications," Proceedings of the 5th IEEE Pulsed Power Conference, 1985.

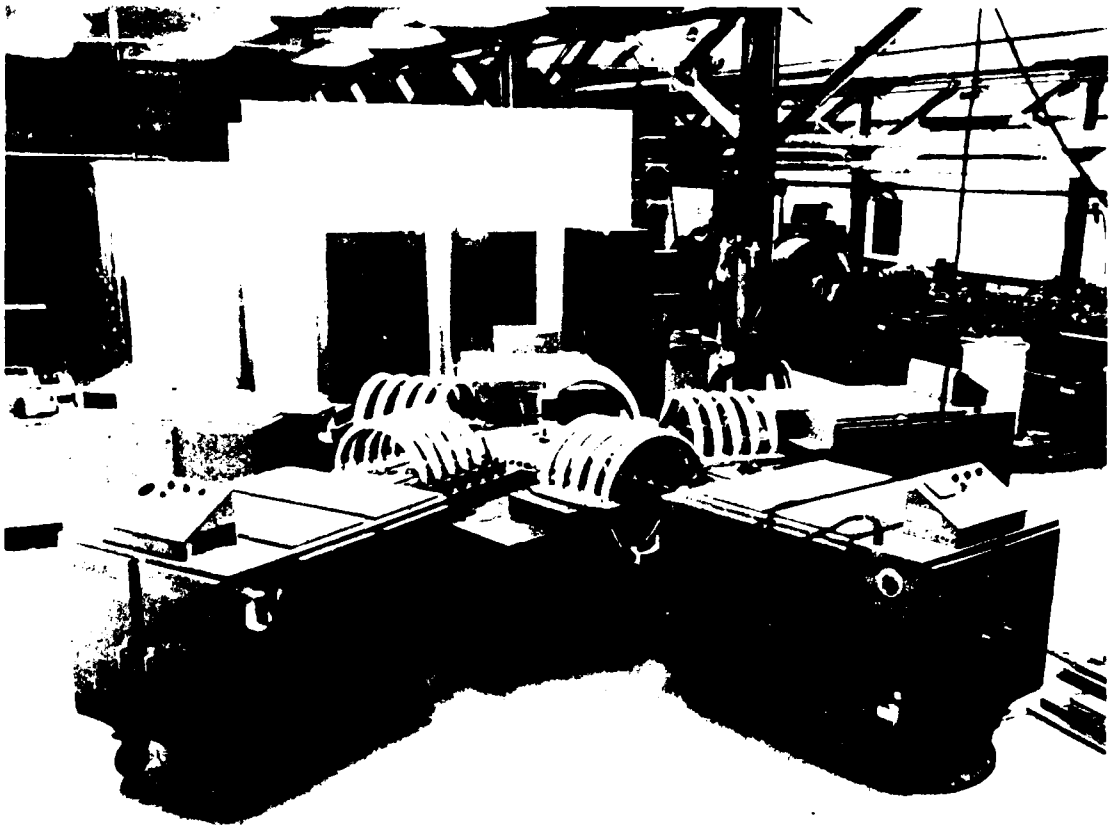

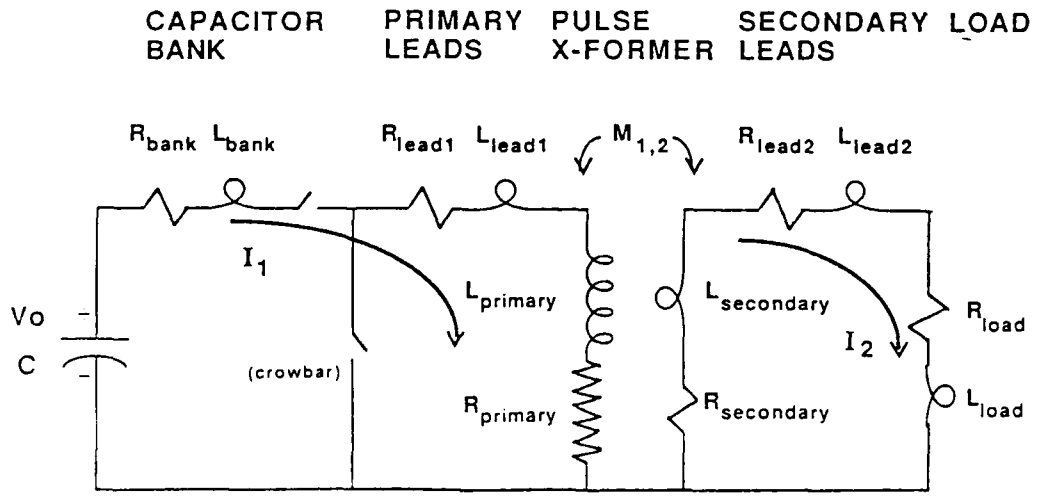

Figure 1. Photograph of CAPSTAR and Equivalent Circuit for Pulse Transformers.

load which comprises an arbitrary inductance and resistance. Summing voltages around the right and left hand loops by Kirchoff's Law yields:

$$V_{cap} = I_1(R_{bank}+R_{lead1}+R_{pri}) + \frac{dI_1}{dt}(L_{bank}+L_{lead1}+L_{pri}) + \frac{dI_2}{dt} M_{1,2} \qquad (1)$$

and

$$0 = I_2(R_{sec}+R_{lead2}+R_{load}) + \frac{dI_2}{dt} (L_{sec}+L_{lead2}+L_{load}) + \frac{dI_1}{dt} M_{1,2} , \qquad (2)$$

where $M_{1,2}$ is the mutual inductance between the primary and secondary circuits. From Eq. 2,

$$\frac{dI_2}{dt} = \frac{-I_2 (R_{2tot}) - (dI_1/dt) M_{1,2}}{L_{2tot}} \qquad (3)$$

where

$$L_{2tot} = L_{sec} + L_{lead2} + L_{load}$$

and

$$R_{2tot} = R_{sec} + R_{lead2} + R_{load} \quad .$$

Substituting into Eq. (1)

$$\frac{dI_1}{dt} = \frac{V_{cap} - I_1 R_{1tot} + (M_{1,2} I_2 R_{2tot}/L_{2tot})}{L_{1tot} - (M^2_{1,2}/L_{2tot})} \qquad (4)$$

where

$$L_{1tot} = L_{bank} + L_{lead1} + L_{pri}$$

and

$$R_{1tot} = R_{bank} + R_{lead1} + R_{pri} \quad .$$

The performance of the circuit may be easily solved numerically by making the substitution $dI/dt \sim = \Delta I/\Delta t$ for small Δt. The initial conditions $I_1 = I_2 = 0$ and $V_{cap} = V_{charge}$ are updated by calculating the current charge and the

capacitor charge. New values for I_1, I_2 and V_{cap} are found iteratively by using Eqs. (3) and (4) with

$$I = I + \frac{dI}{dt}(\Delta t) \tag{5}$$

and

$$V_{cap} = V_{cap} - I_1 \Delta t/C \quad . \tag{6}$$

The time increment, Δt, was decreased until the output did not change. A value of 1 μs was found to be acceptable. A short computer code has been written to solve Eqs. (3)-(6) and is included in the Appendix.

III. TRANSFORMER BEHAVIOR

The pulse transformers described here, and shown in Fig. 2, are similar in geometry to a coaxial transmission line. The center conductor, or primary winding, has radius a, and forms a single continuous helical winding which passes through holes drilled in both secondary output buss bars. The outer conductor, or secondary winding, is formed from tubular sections of thickness (c - b). Each secondary segment end is joined in parallel with buss bar to form the secondary output buss. This configuration produces a step up in current and a step down in voltage from the primary to the secondary side of the transformer. The ratio of the number of turns in the primary to the single turn in the secondary can be used to describe transformer performance only in special cases. Ideally, if the output of the secondary is shorted and the pulse is relatively short, the ratio of secondary current to primary current should equal the turns ratio.

Previous attempts to model the inductance and coupling of the CAPSTAR system and the subscale transformer assumed that the magnetic field was completely enclosed by the space bounded by the inner wall of the secondary tubes.[2] This type of modeling is only applicable for very short time pulses and a shorted secondary. With the addition of any load inductance the current ratio I_2/I_1 is no longer equal to the number of turns, N.

When no load is connected to the transformer, an apparent contradiction arises in the field strength outside the secondary. The secondary tube can be made quite thick to prevent magnetic field from the primary penetrating outside the tube. If, however, one observes no secondary current when primary current is changing, opposite flowing eddy currents must occur on the inner and outer surfaces of the secondary tubes and field will exist outside the secondary even though none has penetrated into the conducting tube wall. In fact, significant magnetic fields are observed outside the secondary at times too short for field to penetrate the wall thickness of the secondary tube. For the purpose of this report, we will neglect eddy current losses in the secondary tubes and assume that they are thin walled.

[2] Zielinski, Alex E., "Design and Testing of a Pulsed Current Transformer," ARDEC Technical Report ARLCD-TR-85005, April 1985.

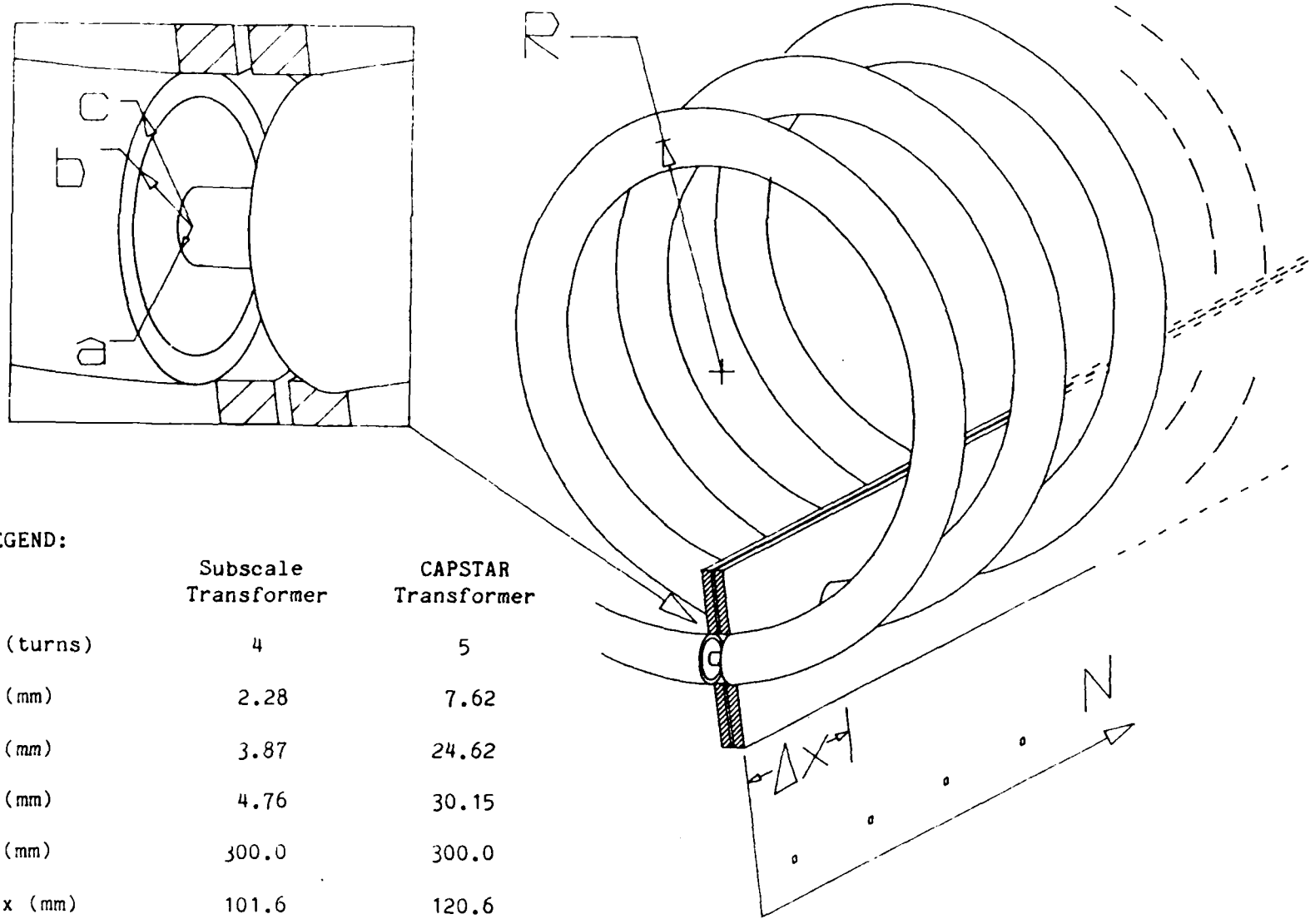

LEGEND:

	Subscale Transformer	CAPSTAR Transformer
N (turns)	4	5
a (mm)	2.28	7.62
b (mm)	3.87	24.62
c (mm)	4.76	30.15
R (mm)	300.0	300.0
Δ x (mm)	101.6	120.6

Figure 2. Transformer Topology.

A. Circuit Inductances

The inductive quantities in our mathematical model are sometimes difficult to measure. For this reason we wish to relate the model parameters to measureable quantities. From Eq. (1), with the secondary open circuited, the inductance seen from the primary terminals, L_{oc}, is equal to the inductance of the primary coil, L_{pri}. Substituting Eq. (3) into Eq. (1), with the secondary short circuited, the inductance seen from the primary terminals, L_{sc}, is:

$$L_{sc} = L_{pri} - M^2_{1,2}/L_{sec} \quad . \tag{8}$$

Substantially all the flux produced by the secondary links the primary and the mutual inductance, $M_{1,2}$, is given by the secondary inductance times N. Substituting in Eq. (8),

$$L_{sc} = L_{pri} - N^2 L_{sec} \quad . \tag{9}$$

Rewriting Eq. (9), the secondary inductance may be expressed solely in terms of measured quantities as

$$L_{sec} = \frac{L_{oc} - L_{sc}}{N^2} \quad . \tag{10}$$

Similarly the coupling constant defined as $k = M_{1,2}/[L_{pri} L_{sec}]^{\frac{1}{2}}$, may also be written in terms of measured quantities as:

$$k = [1 - L_{sc}/L_{oc}]^{\frac{1}{2}} \quad . \tag{11}$$

B. Circuit Resistances

For the primary coil, resistance is calculated based on full current penetration in the winding (DC). This assumption is acceptable because of the filamentary nature of the wire winding. The minimum secondary resistance is calculated from the geometry of the secondary tubes. Again, from Eq. (1), with the secondary open circuited, the resistance seen from the primary terminals, R_{oc}, is equal to the resistance of the primary coil, R_{pri}. Substituting Eq. (3) into Eq. (1) with the secondary shorted, the resistance seen from the primary terminals, R_{sc}, is:

$$R_{sc} = R_{pri} + N^2 R_{sec} \quad . \tag{12}$$

Rewriting in terms of measured quantities:

$$R_{sec} = \frac{R_{sc} - R_{oc}}{N^2} \qquad (13)$$

Since R_{oc} must always be greater than R_{pri}, R_{sec} given in Eq. (13) is somewhat less than actual value.

Equations (10) and (13) show that the secondary impedances referred to the primary side of the current step up transformer are reduced by the square of the turns ratio.

IV. CALCULATED PARAMETERS

A. Circuit Inductances

Shown in Fig. 2 is the geometry used for the pulse transformer. The primary inductance can be calculated from Ref. 3 as,

$$L_{pri} = [.002\ \pi^2\ (R/\Delta x N)\ N^2 K_1] - [.004\ \pi R\ N\ [1.25 - \ln\ (\Delta x/a)] \quad . \qquad (14)$$

Where R is the mean radius of the helical primary coil, Δx is the spacing between turns, a is the radius of the primary conductor, and K_1 is an end effect coefficient given in Ref. 3. From the subscale transformer dimensions L_{pri} = 11.89 μH.

In Ref. (1) the inductance seen from the primary terminals with the secondary shorted was verified to be that of straight coaxial tubes with length $2\pi RN$. This is expressed as:

$$L_{sc} = N\ \mu_o\ R\ [.25 + \ln(b/a)] \quad . \qquad (15)$$

The short circuit inductance calculated from Eq. (15) only includes the magnetic energy of the coaxial configuration. Hence for the subscale transformer:

$$L_{sc} = 1.17\ \mu H.$$

From Eq. (11), the coupling constant is .949. From Eq. (10) the secondary inductance is 670 nH.

B. Circuit Resistance

The DC resistance for the primary coil was calculated based on the handbook value for No. six gauge stranded copper wire as,

$$R' = 1.29 \text{ milliohm/meter}$$

---

[3]Grover, F.W., Inductance Calculations, D. Van Nostrand Co., Inc., NYC, 1946.

giving

$$R_{pri} = 9.7 \text{ milliohms} \quad .$$

The minimum resistance for the secondary tubes (see Fig. 1) may be calculated based on the cross sectional area of conductor which has been penetrated by current as,

$$R_{tube} = 2\pi R/[\sigma(\pi(c^2-b^2)] \quad .$$

The total for all four tubes in parallel is,

$$R_{sec} = 335 \ \mu\Omega \quad .$$

V. MEASURED QUANTITIES

The parameters of interest L_{oc}, L_{sc}, R_{oc} and R_{sc}, are measured as a function of frequency. These inductances are shown in Fig. 3 while the resistances are shown in Fig. 4. For peak current times in the 60 to 100 microsecond range, a frequency of 4000 Hertz was selected to evaluate the inductances. The corresponding open circuit and short circuit inductances are 12.4 μH and 2.11 μH. The measured short circuit inductance does include, however, the output buss of the transformer as well as the inductance of a short composed of a foil. The secondary inductance from Eq. (10) yields 643 nH and the coupling constant, k, from Eq. (11) is .91.

In considering the resistances, it was best to use the lowest possible frequency measurement (100 Hertz). The corresponding open circuit and short circuit resistance are 10.1 milliohms and 13.1 milliohms. The secondary resistance calculated from Eq. (13) yields 188 μΩ.

VI. SIMULATION AND MODEL PERFORMANCE

The circuit model was found to be very useful in understanding the performance of the pulse transformers. The quantities used in the model may be obtained in three different ways: they may be derived from measured quantities as shown in Sec. III; calculated from physical principals as shown in Sec. IV; or derived from iterations of parameter variation to best obtain good agreement between the experiment and transformer model. Departures are made from DC values that are consistent with the circuit geometries and current time dependence.

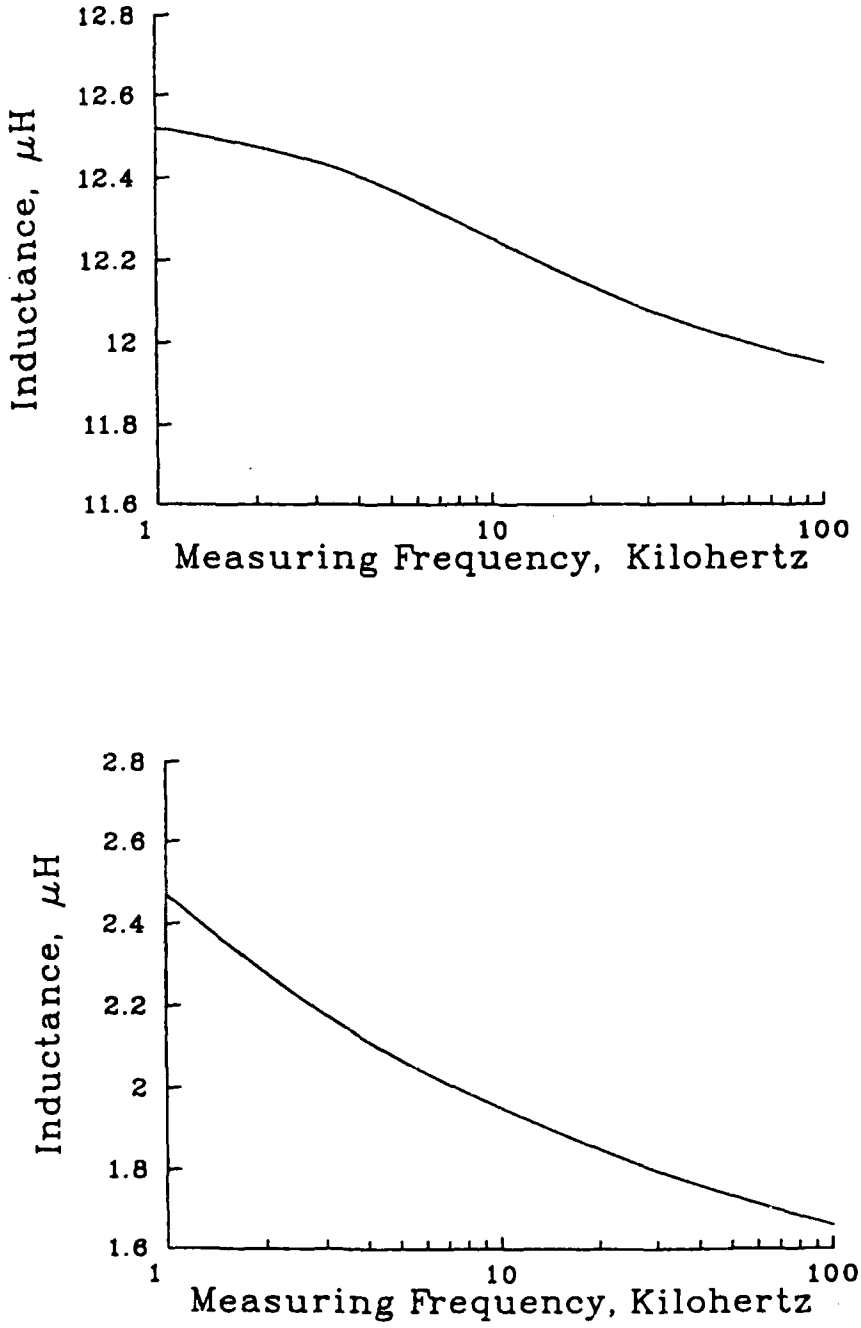

Figure 3. Short (Top Curve) and Open Circuit (Bottom Curve) Circuit Inductance Versus Frequency.

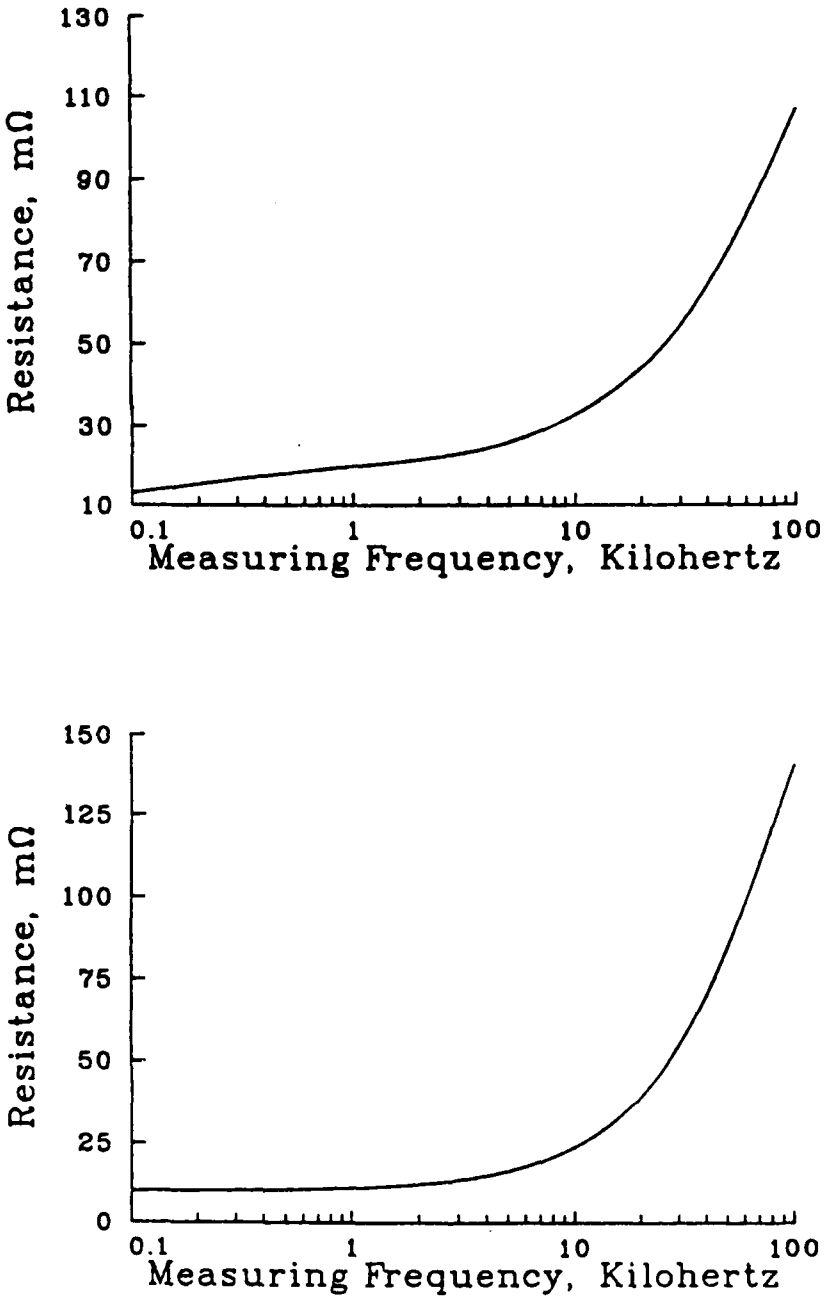

Figure 4. Short (Top Curve) and Open (Bottom Curve) Circuit Resistance Versus Frequency.

A. Subscale Transformer

The first load used to characterize the transformer was a foil short. The load inductance and resistance were measured on a Hewlett Packard LRC Bridge (Model 4274A). Since the foil is thin, the values for inductance and resistance are fairly constant over a wide frequency range. Also, since increasing the load inductance has a major effect on the transformer's performance, the results obtained with the least amount of secondary inductance would best characterize the transformer's behavior. The model capacitor power supply used to pulse the transformer had been characterized previously.[2] All values in the model were adjusted until good agreement between simulation and experimental data were obtained under short circuit conditions. Once the transformer's output could be predicted with a short circuit load of finite inductance and resistance, a one turn coil was used as the secondary load. Again, impedance measurements were made of the load at 4000 Hertz. The simulation was run using the adjusted numbers determined under the short circuit conditions. Figure 5 shows the ratio of primary to secondary currents for the two different load cases. For the coil load case, the model uses a measured resistance at a frequency which corresponds to the time for current to peak (4000 Hertz). From skin depth calculations the current will fully penetrate the coil's cross section at 230 microseconds. Since the load coil's cross sectional dimensions are much greater than the transient skin depth one expects the coil's resistance to be significantly higher at early times and much lower at later times. The effect of the high coil resistance (needed to simulate the experiment at short times) can be seen in Fig. 6. At 150 microseconds the calculated secondary current starts to fall from the experimental curve. This implies that the load resistance used in the calculation is too large for that region of time. The code does not take into account the time dependence of these circuit elements. Table I summarizes the calculated, experimentally measured and the adjusted parameters used for characterizing the subscale transformer circuit.

B. CAPSTAR System

The detailed design and construction for the full scale transformers are presented elsewhere together with some initial test results.[1] Because of the confidence in the circuit model and its validation, the CAPSTAR system was simulated in the same way. The capacitor bank's internal parameters were calculated from experimental data; $L_{bank} \sim 1$ μH and $R_{bank} \sim 10$ milliohms and the crowbar turn on voltage ~ -400 v. As in the subscale pulse transformers testing, a short was used initially to evaluate the transformer's parameters. The inductance and resistance for the secondary common load plate connection were calculated from the voltage drop and secondary dI/dt traces. This was also done for the aluminum short load.

Table II shows the adjusted and calculated parameters used for characterizing CAPSTAR.

Figure 7 shows the amount of magnetic energy transferred to an inductive load for two configurations: One in which the five capacitor banks are used in parallel and one in which they are used in conjunction with the pulse transformers. The cut-off point for use of CAPSTAR to drive an inductive load to maximum energy appears to be 240 nH with 10 μΩ of resistance and, 125 nH with 1000 μΩ of resistance.

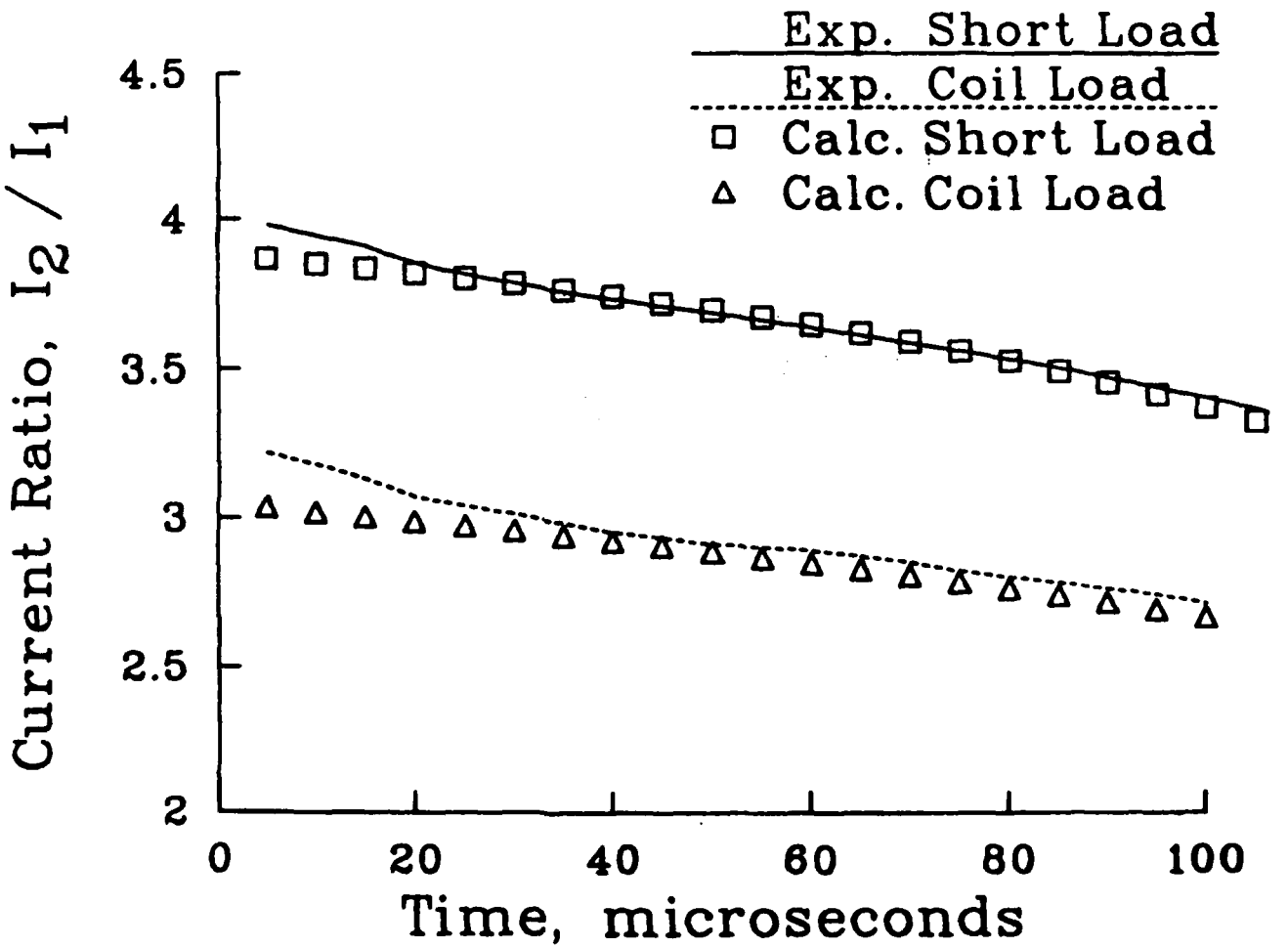

Figure 5. Primary - Secondary Current Ratios for Subscale Transformer.

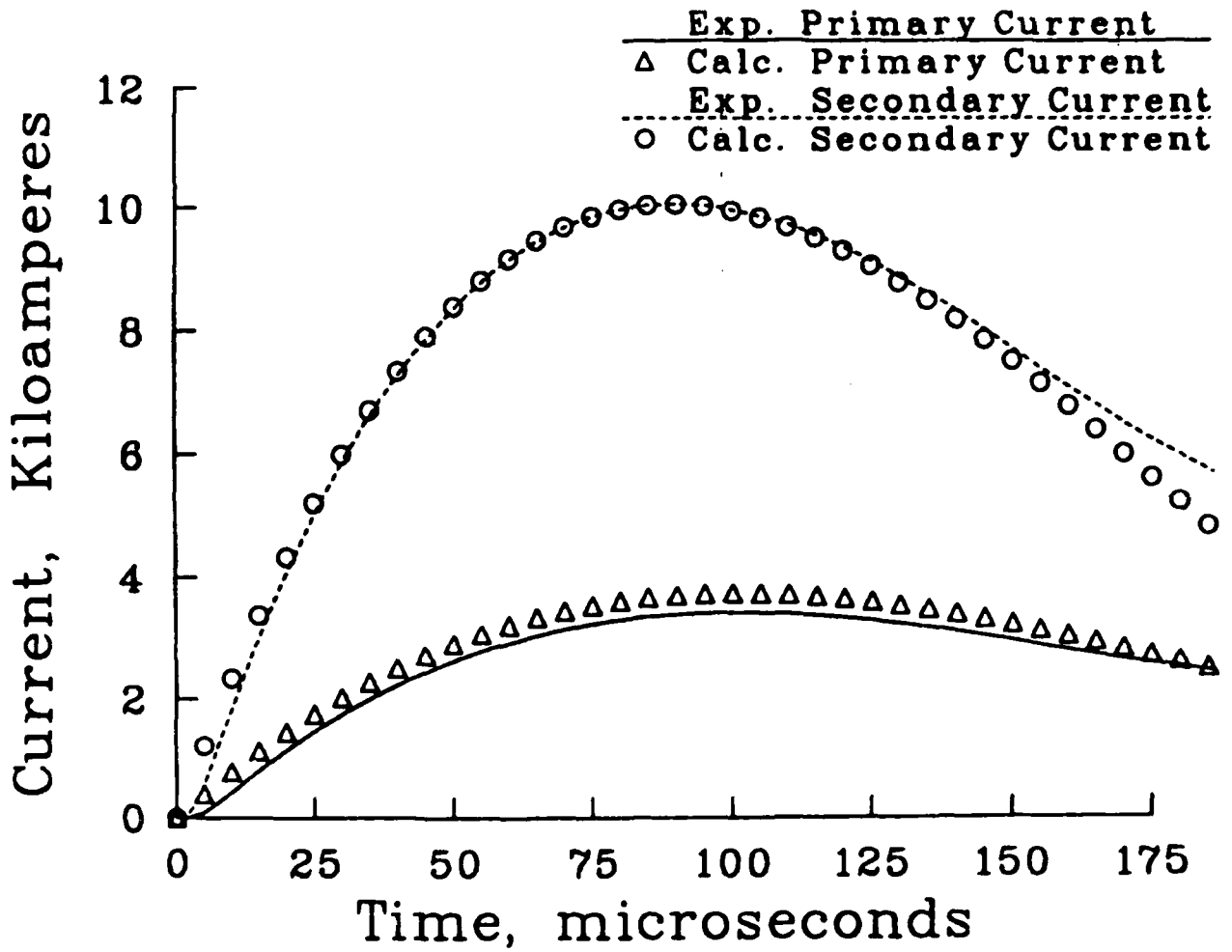

Figure 6. Calculated and Measured Currents for Subscale Transformer (1 Turn Coil Secondary Load).

TABLE I - Subscale Transformer

	CALCULATED	MEASURED	ADJUSTED
Open Circuit Inductance (μH)	11.95	12.4	11.89
Short Circuit Inductance (μH)	1.17	2.11	--
Secondary Inductance (Eq. 10) (nH)	670	643	643
Primary Resistance (mΩ)	9.7	10.1	9.7
Secondary Resistance (μΩ)	335	188	955
Coupling Coefficient (Eq. 11)	.949	.91	.905
Bank Capacitance (μf)	--	1306	1300
Bank Resistance (mΩ)	--	36	36
Bank Inductance (nH)	--	440	440
Load Inductance (nH)	4.48	<4.1>	4.1
Load Resistance (μΩ)	67 (min.)	<60.7>	65

*< > Time Averaged

TABLE II - CAPSTAR

	Calculated	Adjusted
Bank Capacitance (μf)	1100	1050
Bank Inductance (μH)	1.0	1.0
Bank Resistance (mΩ)	10	10
Primary Lead Inductance (nH)	7.2	8.0
Primary Lead Resistance (μΩ)	19.8	20.0
Primary Inductance (μH)	12.89	12.89
Primary Resistance (mΩ)	1.6	1.6
Secondary Inductance (nH)	408.4	375.5
Secondary Resistance (μΩ)	26.0	300.0
Coupling Constant	.89	.853
Load Plate Inductance (nH)	4.46 [<6.2>]	8.5
Load Plate Resistance (μΩ)	5.01 [<4.45>]	5.0
Short Load Inductance (nH)	2.0 [<2.94>]	3.0
Short Load Resistance (μΩ)	4.02 [<5.5>]	5.5

*< > Time Averaged

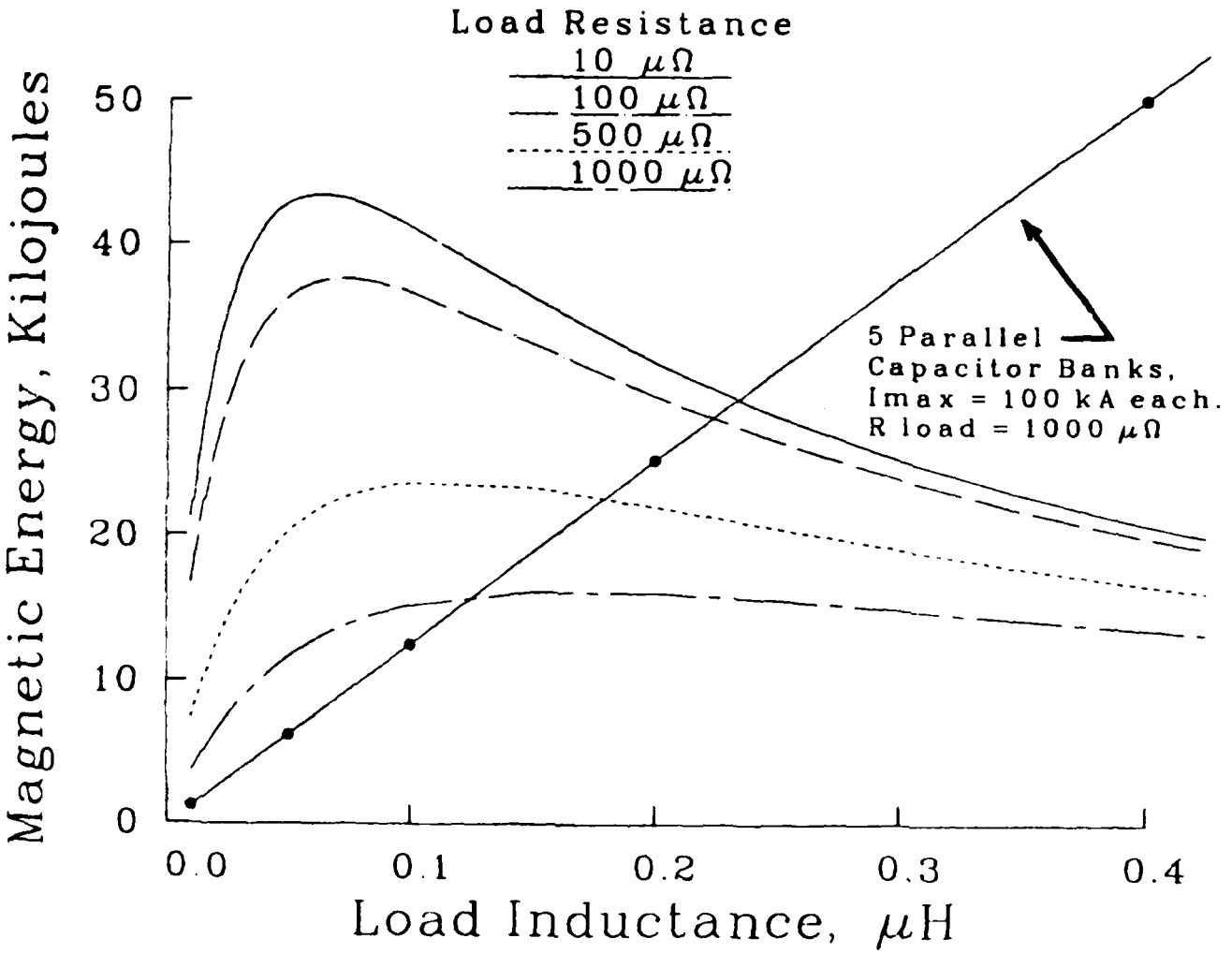

Figure 7. Maximum Load Magnetic Energy Versus Load Inductance.

Defining efficiency as the ratio of maximum delivered magnetic energy to stored electrostatic energy, one finds that CAPSTAR becomes more efficient than the five capacitor banks separately only for loads less than 75 nH with 10 μΩ of resistance and, 25 nH with 500 μΩ of resistance. This is because, with the pulse transformers and any inductive secondary load, the banks can be operated at the maximum charge voltage (10 kv) without going over the maximum current rating (100 kA). This is not the case when the capacitor banks are used separately. The maximum current rating for use with low inductive loads is reached with charge voltages much less than 10 kv.

The goal of the CAPSTAR system was to electromagnetically stress a composite round bore railgun barrel section. One such barrel had a measured time averaged inductance and resistance gradient of .374 μH/m and 964 μΩ/m, respectively.[4] Assuming that the inductance gradient has no dependence on the bore radius, and that the resistance gradient scales as one over the bore radius, then suitable barrel dimensions can be found to achieve a peak barrel pressure. Barrels with lengths of at least two bore dimensions are only considered. Figure 8 illustrates how the barrel length limits the maximum peak pressure for a given bore diameter. This graph is for the CAPSTAR system at full-rated voltage. The time for the pressure to reach its peak for the CAPSTAR parameters in Fig. 8 is in the range of 40-100 microseconds. This type of pressure profile may be more severe than that experienced by a railgun barrel when driving a railgun armature.

Experimental and calculated data of currents and current ratios with a barrel load are shown in Figs. 9 through 11. Because of the size of the CAPSTAR system, the data was not as abundant as that taken on the subscale transformer. Only one out of the five capacitor banks was instrumented; measured quantities included the primary-side voltage (outside the capacitor bank) and the primary dI/dt. Since the charge voltage on every bank is set by a separate potentiometer there was some uncertainty in the value of the initial charge voltage. One way to determine the initial charge voltage is to add the capacitor bank's internal impedance drop to the measured peak primary-side voltage. As a result, there is uncertainty due to the unknown contribution of current from the remaining four transformers. In the model it was assumed that all five capacitor banks were charged to the same initial value and each transformers' secondary output supplied 1/5 the total load current.

VII. PROJECTED PERFORMANCE WITH RAILGUN LOADS

In addition to modeling the pulse transformer with constant inductive and resistive secondary loads, it was thought to model the CAPSTAR system with a variable load such as a railgun with a moving armature. A solid armature would contribute a smaller loss than a plasma armature, but would have to maintain it's mechanical integrity throughout the high secondary current pulse. The armature used in the simulation is assumed to be solid and lossless. Although this is not an attempt to optimize a railgun to a pulse transformer it does provide some insight into currents and velocities attainable. In order to assess the CAPSTAR power source driving a railgun load, the 5 capacitor

[4] Laboratory Notebook No. LCA 375, ARDEC, Picatinny Arsenal, Dover, N.J.

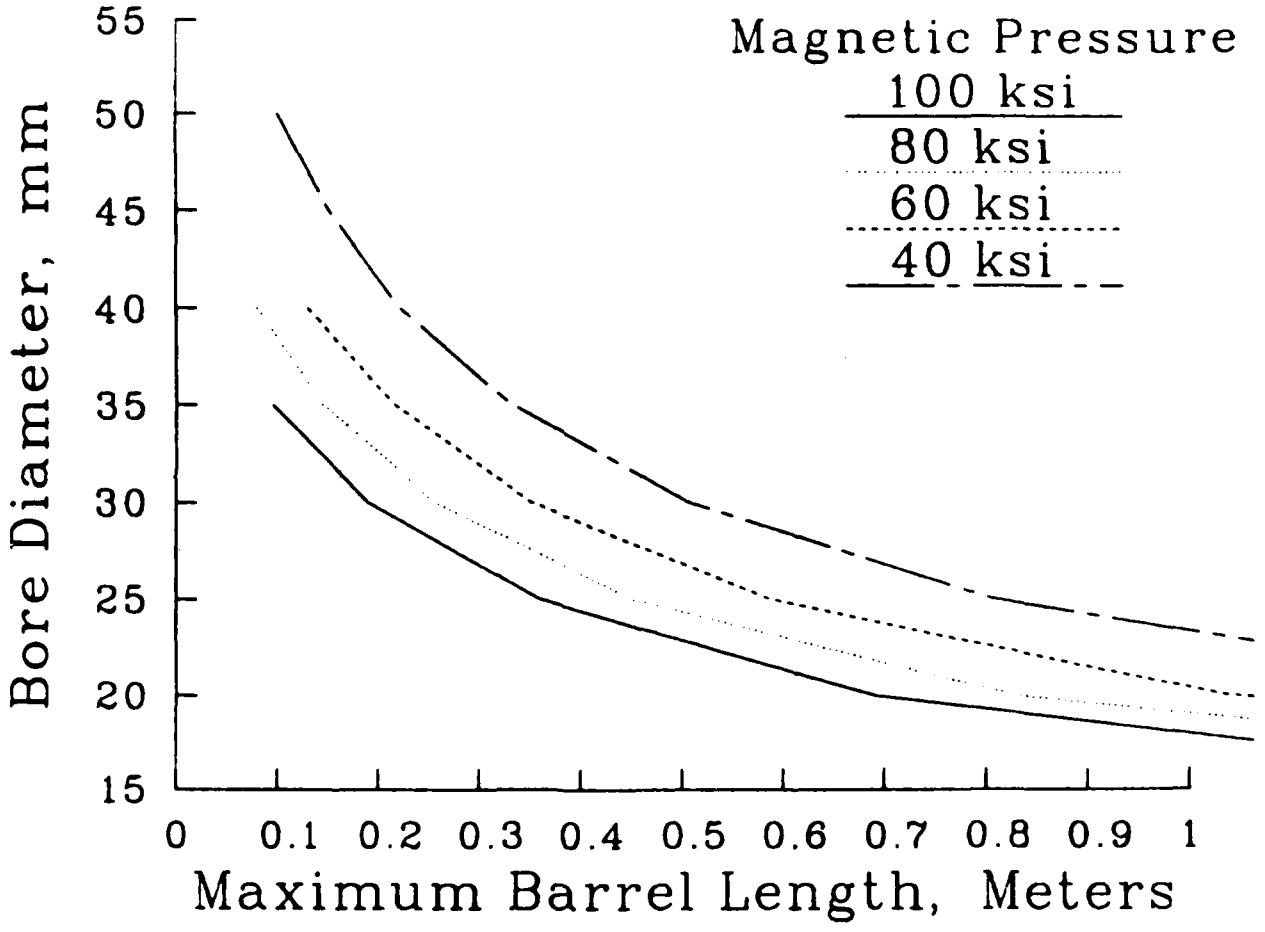

Figure 8. Bore Diameter Versus Maximum Barrel Length (1 ksi = 6.894 MPa).

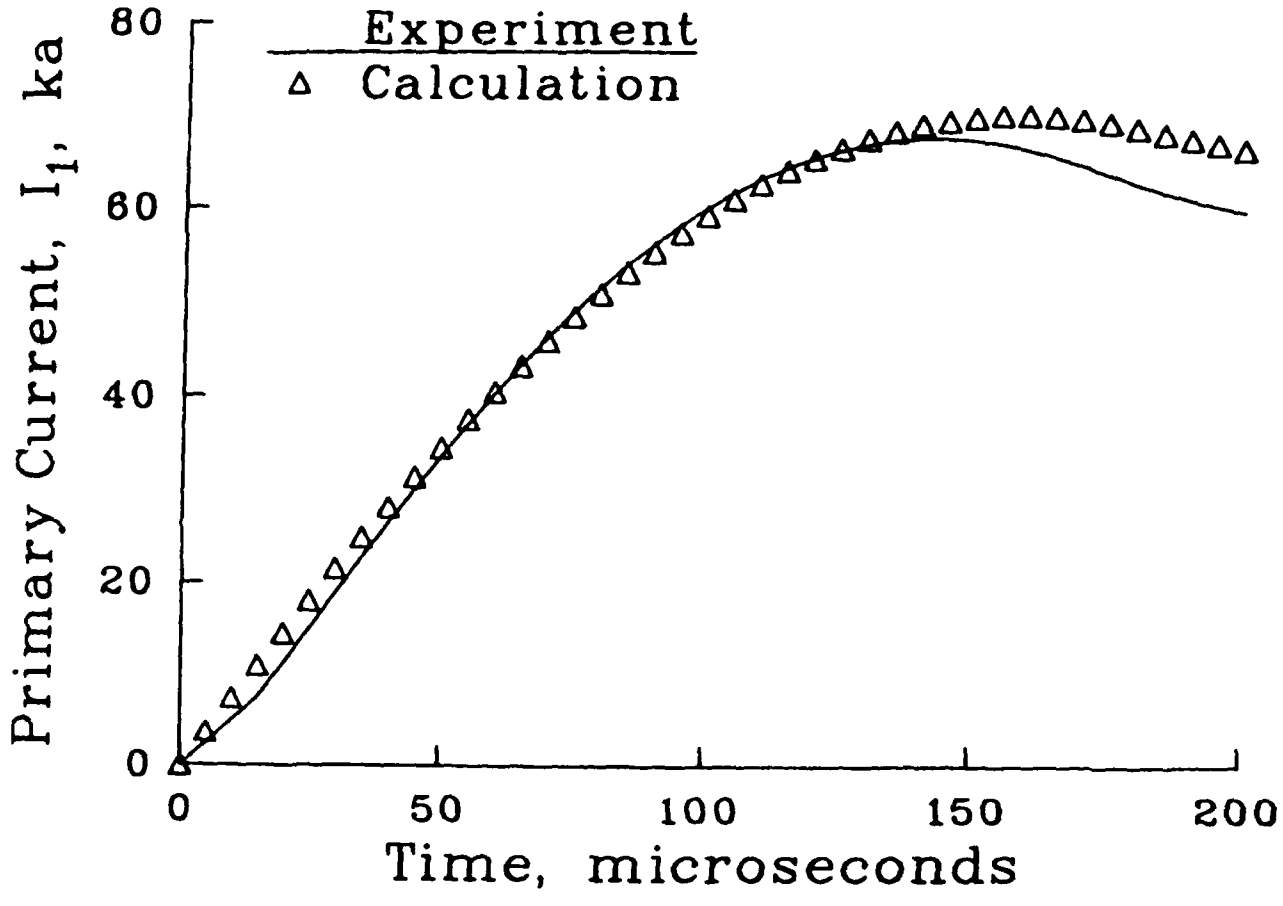

Figure 9. Calculated and Measured Primary Current for CAPSTAR With a Barrel Load (One Transformer).

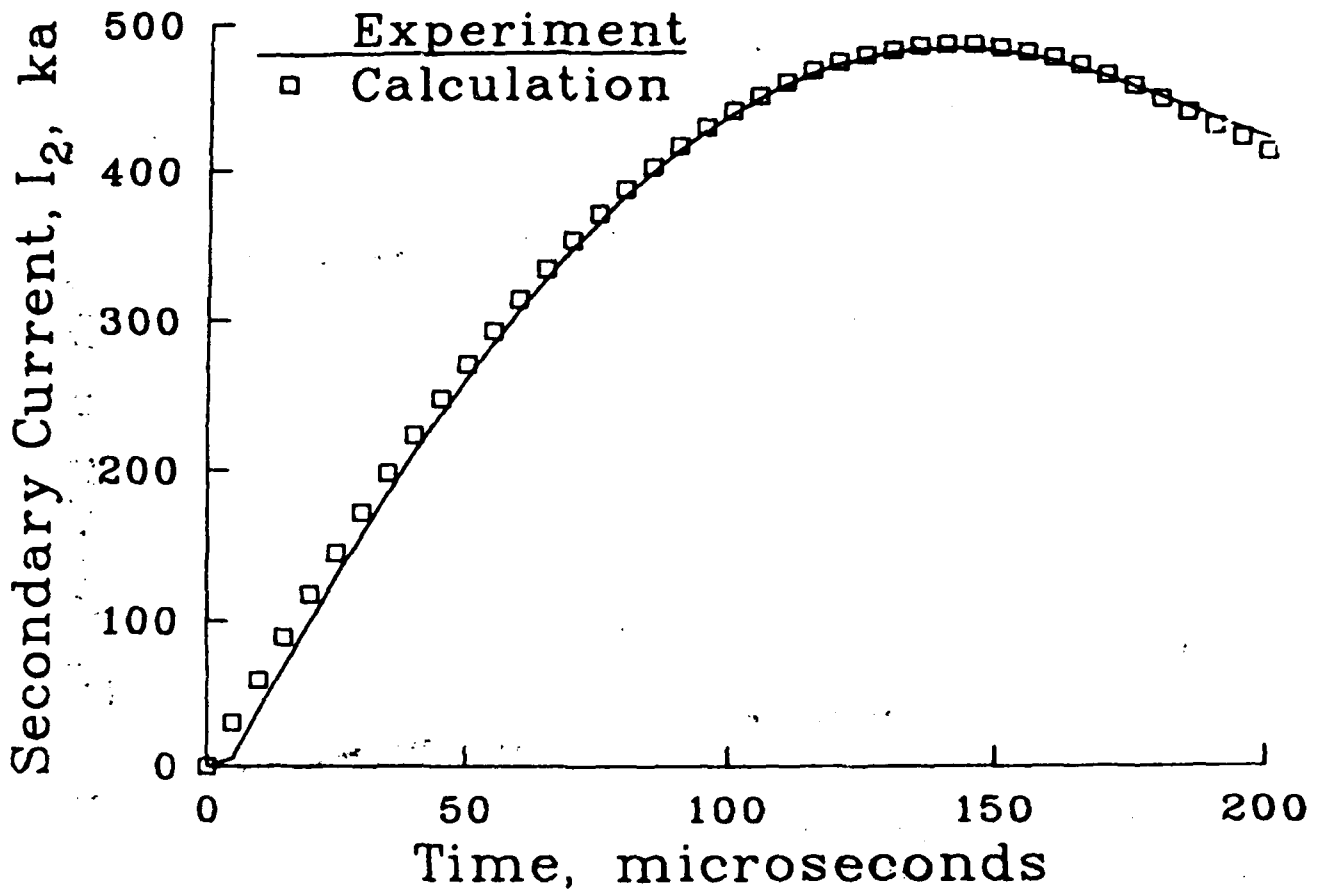

Figure 10. Calculated and Measured Barrel Load Current for CAPSTAR.

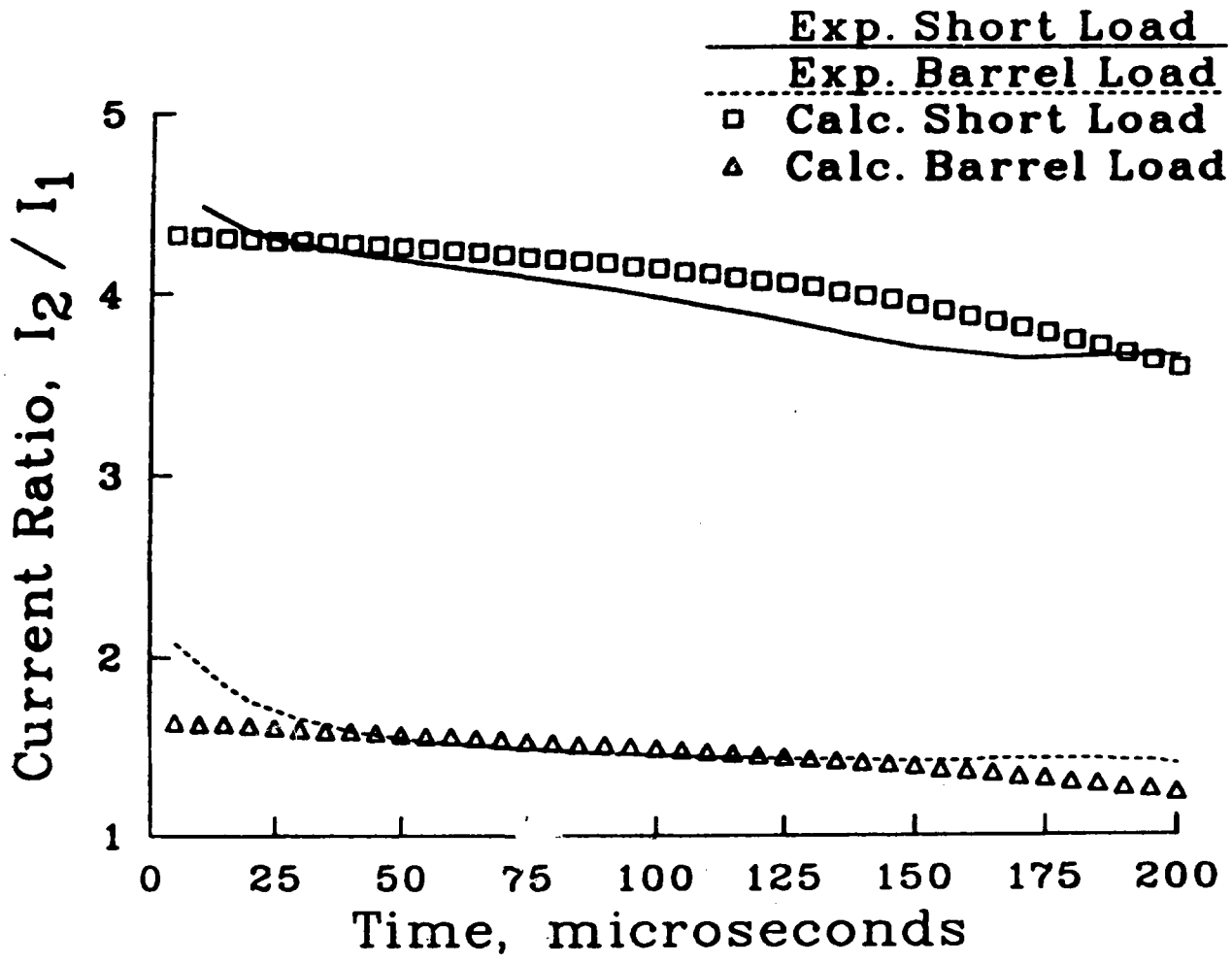

Figure 11. Primary - Secondary Current Ratios for CAPSTAR.

banks in parallel are used as a reference point. Since the maximum current output of each bank is 100,000 amperes, a 1.4 μH inductor with a 20 millisecond time constant is used to current limit the banks at the maximum charge voltage of 10,000 volts. This will produce a maximum load current of .5 Megamp. A 12.7 mm square bore, 1 meter long railgun barrel is used as the secondary load. The resulting pressure waveforms for both power sources are shown in Fig. 12. The launch package mass for both configurations is 3 grams. The velocity for each of these two power sources is shown in Fig. 13. The transformers work quite well in multiplying the primary current even with a railgun load; however, the launch structure still has to contain the high peak pressure. For the load currents that can be produced by CAPSTAR power source an acceptable bore size that limits the peak pressure to approximately 40,000 psi is 60 mm. Correspondingly, for the same pressure, the bore size for the 5 parallel banks is 15 mm. The minimum Lexan launch package mass for the 60 mm bore is roughly 250 grams. The mass was varied around that point and this variation is plotted against the velocity obtained using both power sources in Fig. 14.
It can be seen that CAPSTAR power source can be best utilized to drive a large bore railgun. This is solely to limit the bursting pressure to an acceptable level. Correspondingly, large projectiles can be launched. The heavy launch mass keeps the load inductance and resistance quite low early in the current rise. This allows the current ratio to remain close to the number of turns. After the armature has moved some distance the barrel load inductance (L'z) and load resistance (R'z + L'v) reduce the coupling. This can be seen in Fig. 15. Similarly, the secondary currents are shown in Fig. 16. Also, shown in Fig. 16 is a railgun driving a 200 volt drop plasma armature. The velocities attained are of no consequence for bore size less than 60 mm since it is doubtful whether a barrel could contain the high pressures produced by the CAPSTAR power source. Since the pressure pulse has a high peak and a relatively short width, short barrel lengths (300 mm) could be used as a railgun load. Peak to average accelerations of 4 are obtainable.

VIII. CONCLUSION

We have developed and tested a model for a capacitor driven, air core pulse transformer. The model has been verified on both the subscale transformer and with preliminary data from the CAPSTAR system. Knowing the initial capacitor bank voltage in the CAPSTAR system proved to be the greatest source of uncertainty in matching the simulation to the experiment. One of the most significant findings is that the load impedance must be quite small if the current ratio is expected to approach the turns ratio. For EM launcher components the self inductance is often too large for the pulse transformers to be beneficial. This is evident from the fact that EM launchers generally must store significant amounts of magnetic field energy in order to perform useful work. Furthermore, any great effort spent in enclosing the primary in very thick walled tubing to contain the magnetic field simply makes the transformer heavier without necessarily improving performance. The equivalent circuit model does not take into account the eddy current losses in the secondary tubes. For very high impedance loads we expect these losses to be significant and should be included in future modeling.

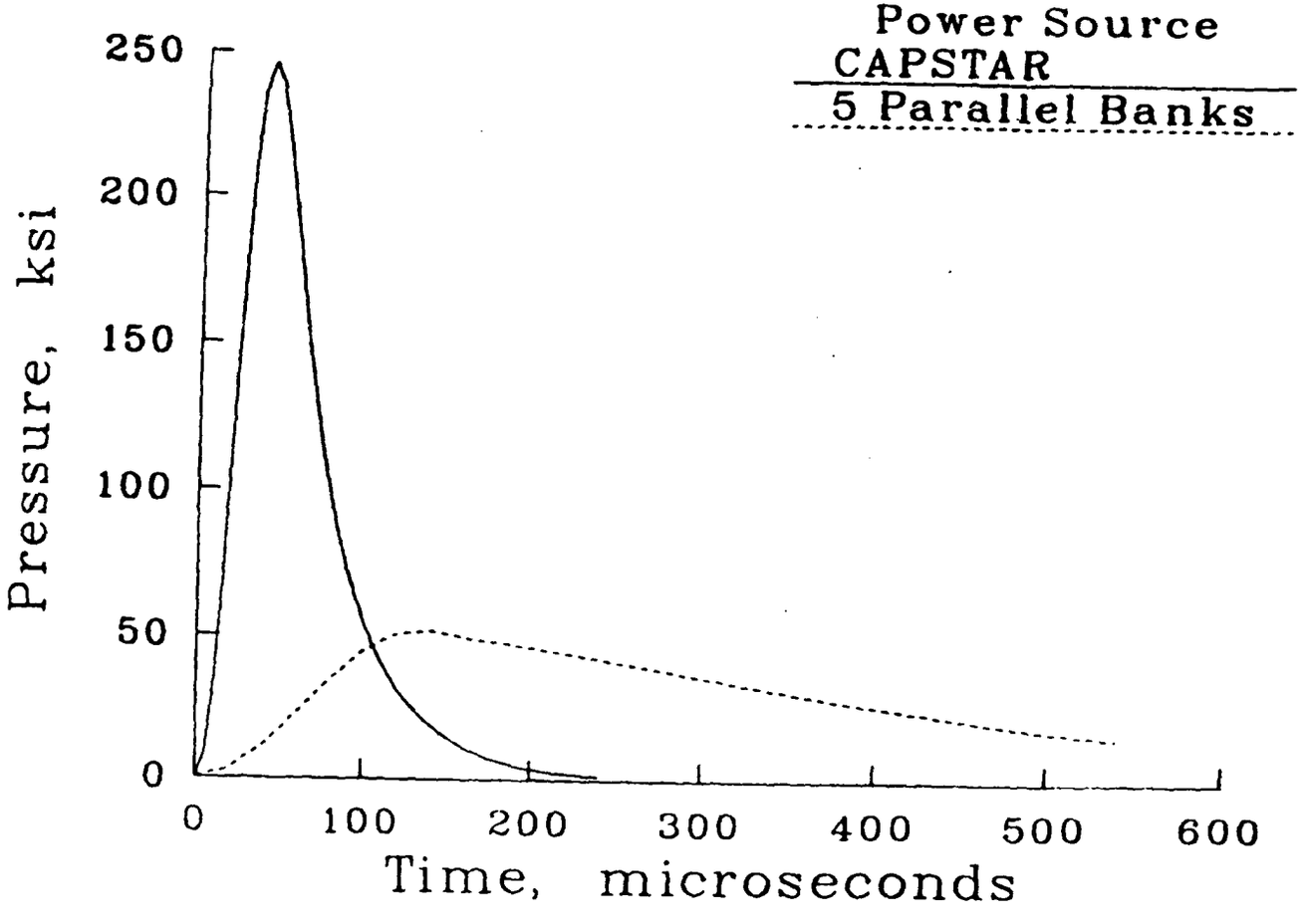

Figure 12. Barrel Pressure Simulation for Two Different Power Sources (1 ksi = 6.894 MPa).

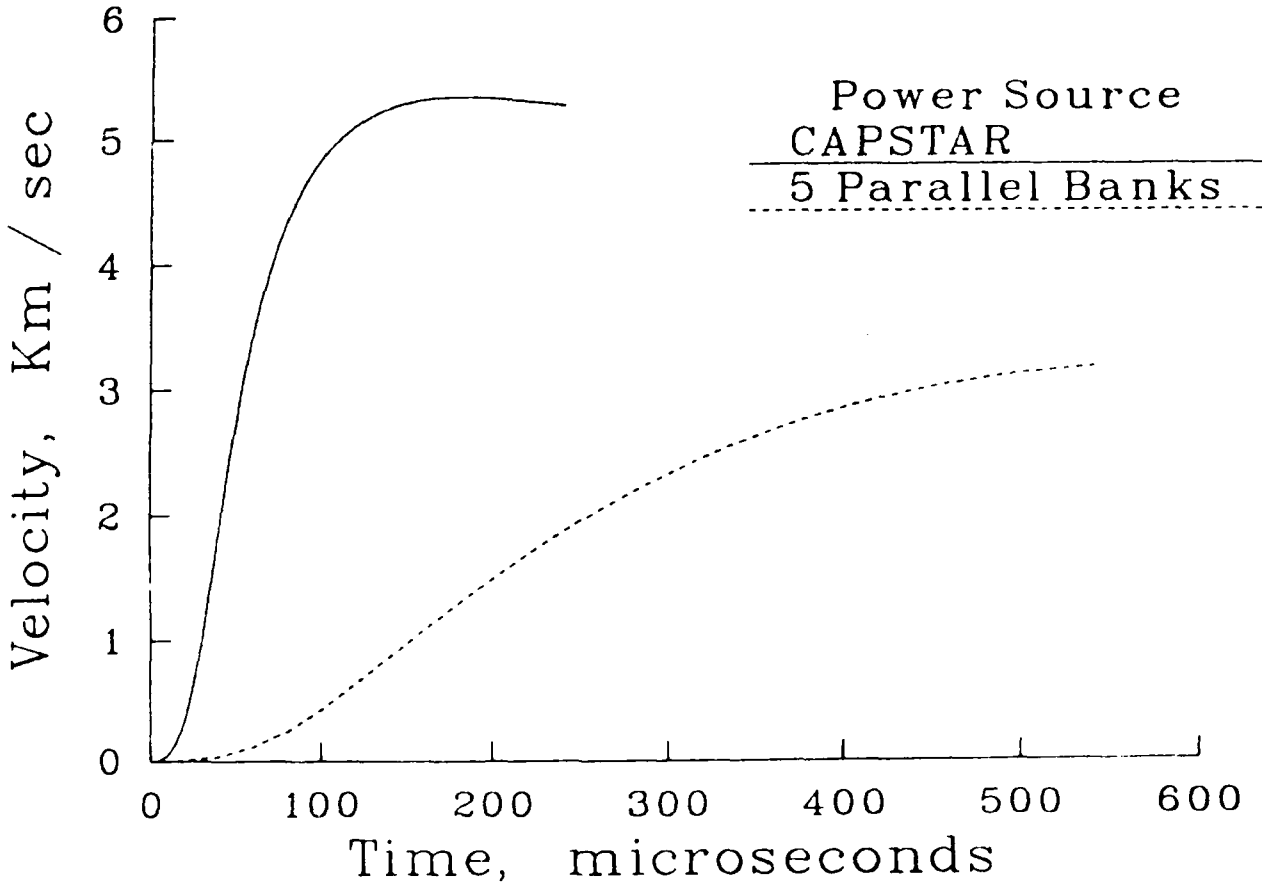

Figure 13. Velocity Simulation for Two Different Power Sources.

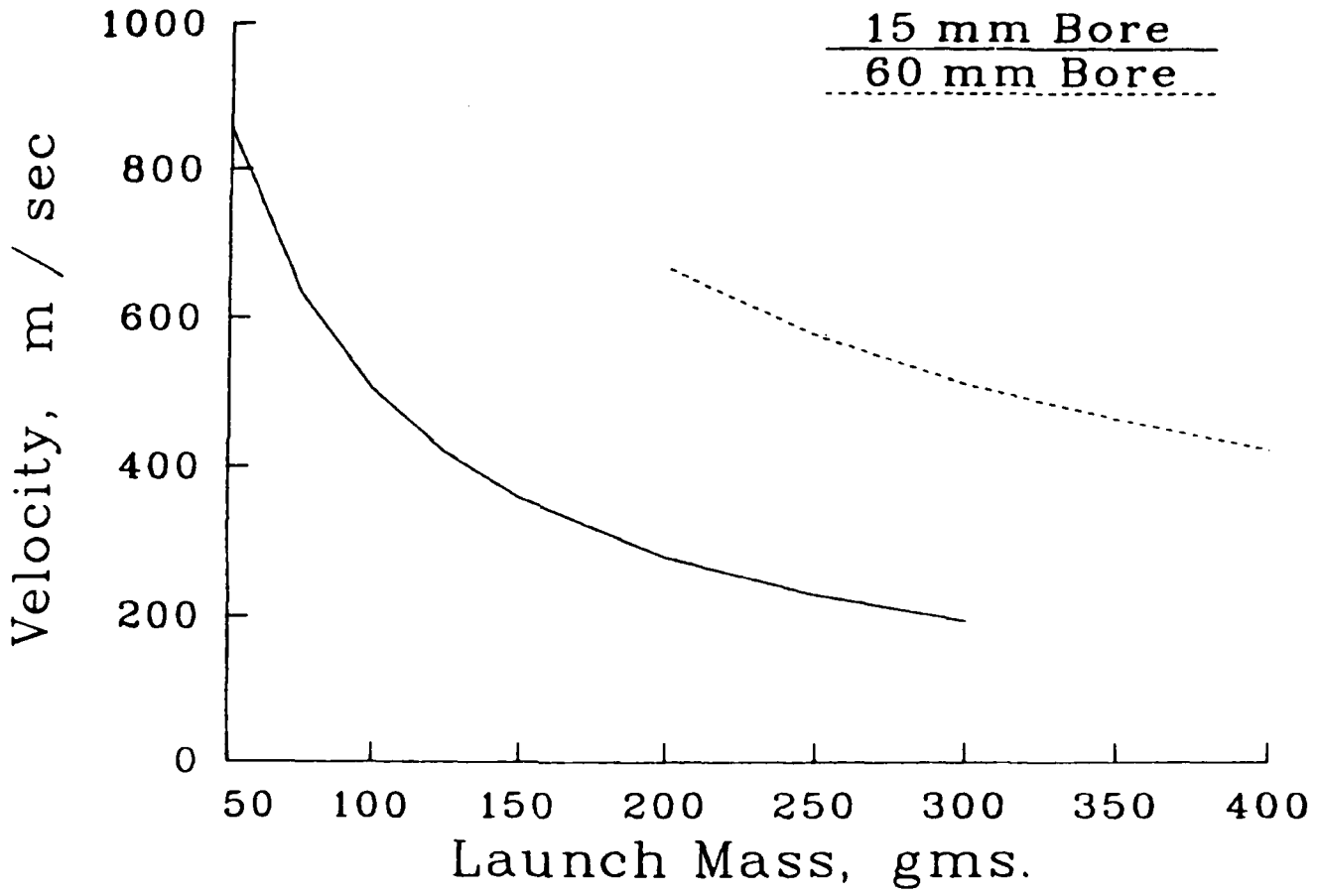

Figure 14. Velocity Versus Mass for Two Different Bore Sizes.

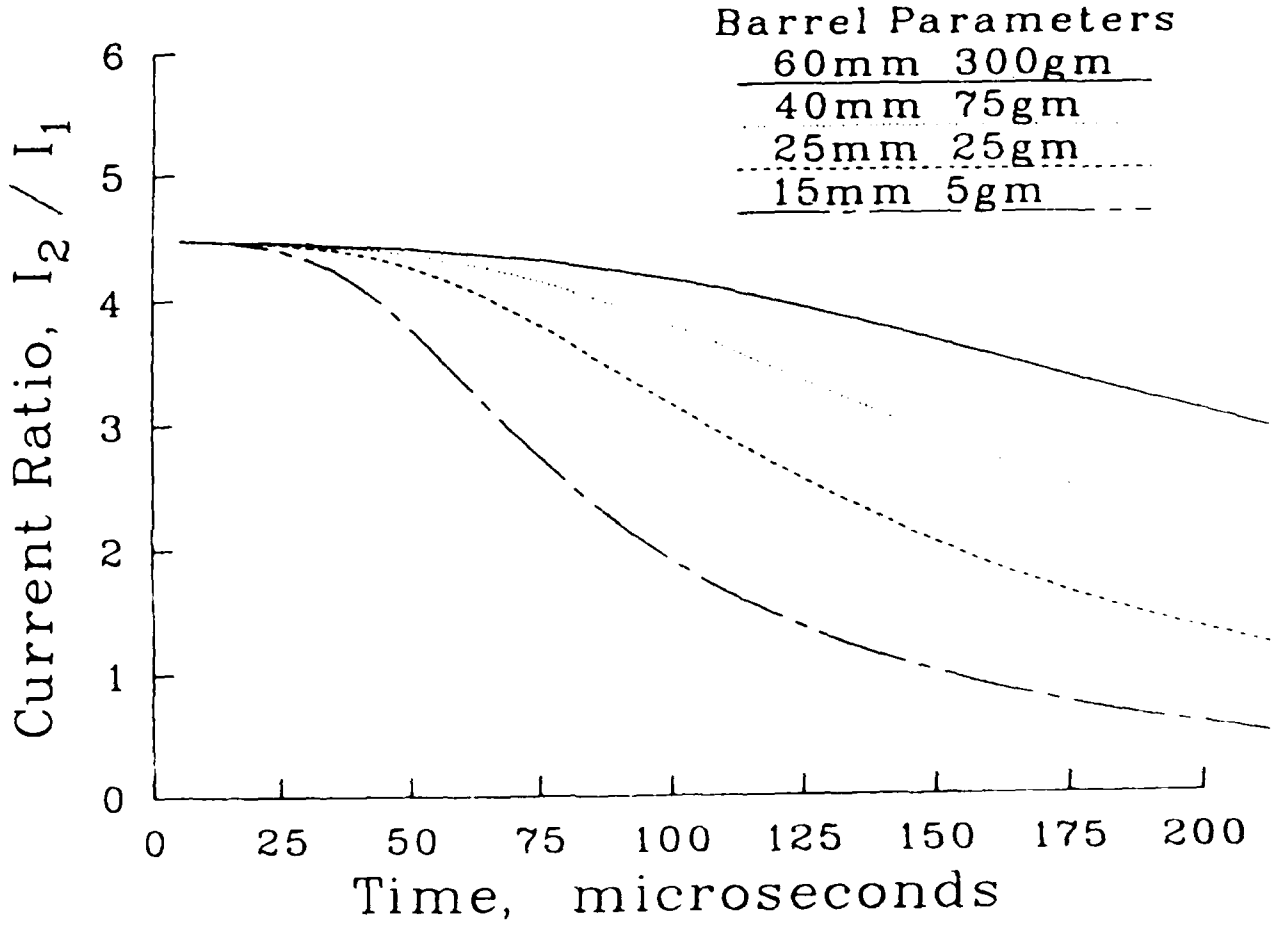

Figure 15. CAPSTAR Current Ratio Versus Time for Different Barrel Parameters.

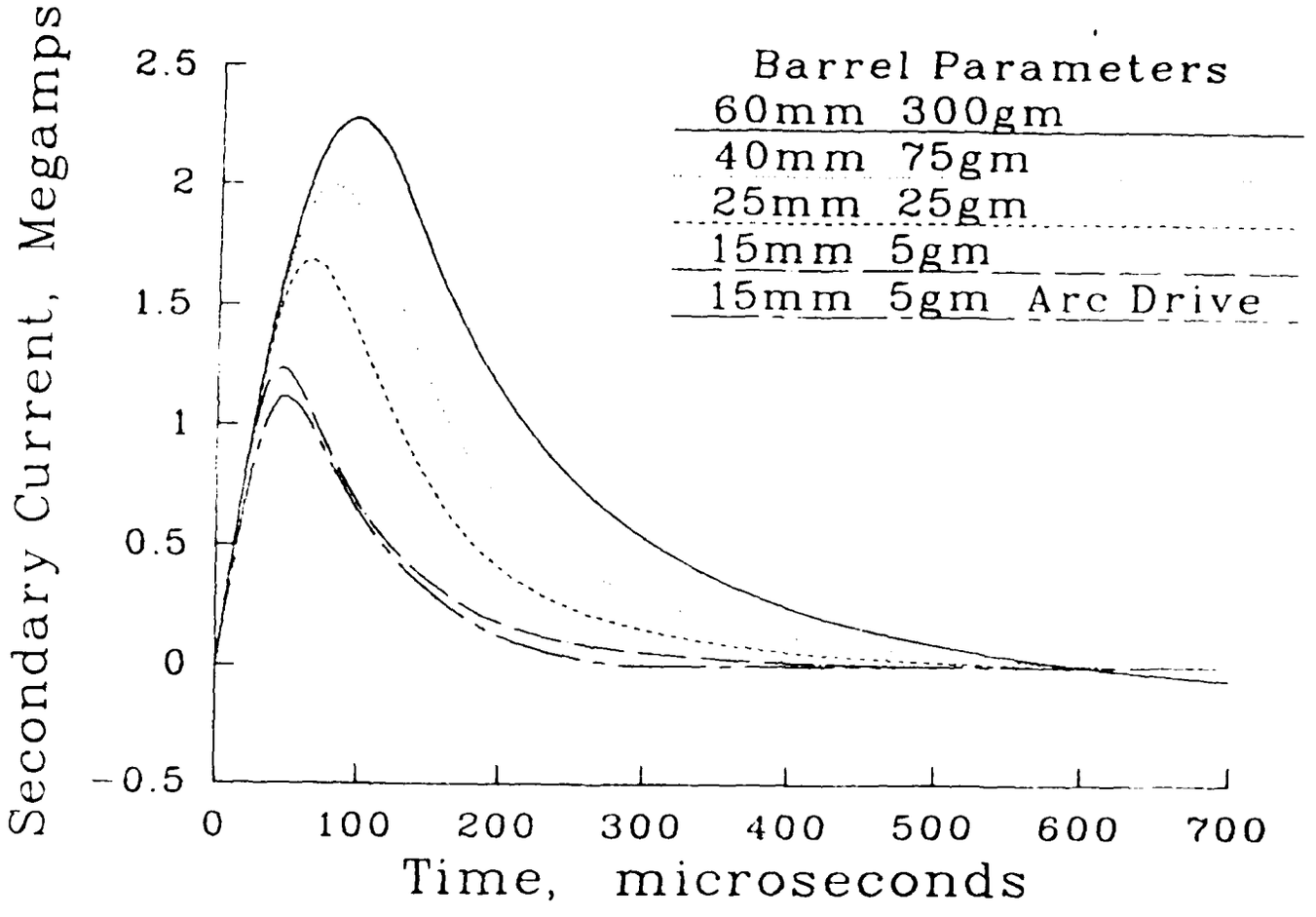

Figure 16. CAPSTAR Secondary Currents Versus Time for Different Barrel Parameters.

With the verified transformer model, we have undertaken a brief study of the use of pulse transformers directly driving railguns as a load. Our findings show that the transformers are worthwhile only for short times and for correspondingly short barrel lengths. The maximum utility of the pulse transformers appears to be in applying strong magnetic forces to low inductance structures for very short times. When the power source switchgear or an internal impedance limits the maximum current, the pulse transformers will provide much larger peak currents if the load is carefully chosen and the transformer losses are acceptable.

REFERENCES

1. Pappas, J.A., Driga, M.D. and Weldon, W.F., "High Current Coaxial Pulse Transformer for Railgun Applications," Proceedings of the 5th IEEE Pulsed Power Conference, 1985.

2. Zielinski, Alex E., "Design and Testing of a Pulsed Current Transformer," ARDEC Technical Report ARLCD-TR-85005, April 1985.

3. Grover, F.W., Inductance Calculations, D.Van Nostrand Co., Inc., NYC, 1946.

4. Laboratory Notebook No. LCA 375, ARDEC, Picatinny Arsenal, Dover, NJ.

APPENDIX

COMPUTER PROGRAM

```
10 REM ARDEC PULSE [illegible]
40 PRINT"THIS PROGRAM [illegible]
50 PRINT"SCALE PULSE [illegible]
60 REM INPUTED PARAMETERS
70 REM INITIAL CAPACITOR VOLTS
75 V#=0
80 VCAP=5000.0
90 REM CAPACITANCE
100 CAP=.30525
110 REM CROWBAR VOLTAGE
120 CROWBR=-400.00
125 Vcrbr=0.0
130 REM BANK RESISTANCE
140 RBANK=.002
150 REM BANK INDUCTANCE
160 LBANK=.20E-6
170 REM PRIMARY LEAD INDUCTANCE
180 LO=1.6E-09
190 REM PRIMARY LEAD RESISTANCE
200 RO=4.0E-6
210 REM PULSE TRANS PRIMARY INDUCTANCE
220 LPRI=2.57E-6
230 REM PULSE TRANS PRIMARY RESISTANCE
240 RPRI=320E-6
250 REM PULSE TRANS SECONDARY INDUCTANCE
260 LSEC=75.10E-9
270 REM PULSE TRANS SECONDARY RESISTANCE
280 RSEC=60.0E-06
290 REM SECONDARY LEAD INDUCTANCE
300 L2=8.5E-09
310 REM SECONDARY LEAD RESISTANCE
320 R2=5.0E-06
330 REM SECONDARY LOAD INDUCTANCE
340 LL=144.0E-09
350 REM SECONDARY LOAD RESISTANCE
360 RL=360.0E-06
370 REM COUPLING COEFFICIENT
380 K=.853
390 REM TIME INTERVAL
400 DT=1.0E-6
405 REM PRINT INTERVAL;EVERY PT'TH CAL
407 PT=5.00
410 REM FINAL TIME
420 TF=200E-6
424 REM AVOIDS ROUDOFF ERROR IN TIME
425 TD=0
427 Icur=0\ Iprev=0
430 PRINT\ PRINT
440 I$="PRICUR"\ I$="[illegible]"
445 R1$="RATIO"\ R1=0\ V1=0
447 I1$="amps"\ V$="volts"
450 T=0\ I1=0\ I2=0\ V=[illegible]
```

```
    imag$="###.#   ##.##^^^^   ##.##^^^^   ##.##^^^^   ##.##^^^^      #.##"
450 M=K*SQR(LPRI*LSEC)\ N1=0
470 PRINT USING"'RRRR    'RRRR      'RRRRRR     'RRRRRR     'RRRRR"&
    +"       'RRRRR",T1$,V5$,I5$,I6$,V6$,R1$
480 PRINT USING"'RRRR    'RRRRR       'RRRR      'RRRR       'RRRRR"&
    +"      'RRRRR",T$,V$,I1$,I1$,V$,R$
490 print using imag$,t,v,i,i,i,i
510 GOSUB 1300
    IF T>TF GOTO 2000
530 IF N1/PT<>1.0 GOTO 600
540 REM PRINTING ROUTINE LINES 530-590
550 TD=TD+PT
560 PRINT USING imag$,TD,V,I1/5,I2,VL,R1
580 REM RESET PRINTING COUNTER
590 N1=0.00
    GOTO 510
600 goto 2000
1000 REM CIRCUIT EQUATIONS SUBROUTINE
1005 Iprev=-I2
1010 T=T+DT
1020 N1=N1+1.00
1030 REM TOTAL PRIMARY INDUCTANCE
1040 L5=L0+LBANK+LPRI
1050 REM TOTAL SECONDARY INDUCTANCE
1060 L6=LSEC+LL+L2
1070 REM TOTAL PRIMARY RESISTANCE
1080 R5=R0+RBANK+RPRI
1090 REM TOTAL SECONDARY RESISTANCE
1100 R6=RSEC+RL+R2
1110 DENOM=L5-(M^2/L6)
1115 If I1=0.0 Then Vosc=1.0\ Goto 1120
1117  Vosc=I1/abs(I1)
1120  D1=(Q/CAP-I1*R5+(Verbr*Vosc)+M*I2*R6/L6)/DENOM
1130 D2=-(I2*R6+M*D1)/L6
1140 I1=I1+D1*DT
1150 I2=I2+D2*DT
1160 Icur=-I2
1170 If Icur>Iprev Then I2max=Icur\ Tpk=T
     VL=I2*RL+D2*LL
1180 R1=-I2/I1
1184 IF V9=1 GOTO 1190
1185 Q=Q-I1*DT
1187 V=Q/CAP
1188  IF (1-(V/CRBR)<=0) THEN Verbr=-200\ RBANK=0.0\ LBANK=0\ V9=1
     RETURN
     Print"The maximum secondary current was";I2max/1e3;" kiloamperes, at";&
     +Tpk*1e6;" microseconds"
     END
```

DISTRIBUTION LIST

No. of Copies	Organization
2	Administrator Defense Technical Info Center ATTN: DTIC-FDAC Cameron Station, Bldg 5 Alexandria, VA 22304-6145
10	CIA DIR/DB/Standard GE47 HQ Washington, DC 20505
1	HQDA ATTN: DAMA-ART-M Washington, DC 20310
1	Commander US Army Armament RD&E Center ATTN: SMCAR-MSI Dover, NJ 07801-5001
1	Commander US Army ARDEC ATTN: SMCAR-TDC Dover, NJ 07801
1	Commander US Army RD&E Center ATTN: SMCAR-SCA-E, Mr. H. Kahn Dover, NJ 07801-5001
2	Commander US Army RD&E Center ATTN: SMCAR-LCA-C Mr. John A. Bennett Dr. Thaddeus Gora Dover, NJ 07801-5001
1	Commander US Army Materiel Command ATTN: AMCDRA-ST 5001 Eisenhower Avenue Alexandria, VA 22333-0001
2	Director US Army Missile Command ATTN: AMSMI-YDL Redstone Arsenal, AL 35898-5500
2	Commander US AMCCOM ARDEC CCAC Benet Weapons Laboratory ATTN: SMCAR-CCB-TL SMCAR-LCB-DS, Dr. C.A. Andrade Watervliet, NY 12189-4050
1	Commander US Army Armament, Munitions & Chemical Command ATTN: AMSMC-IMP-L Rock Island, IL 61299-7300
1	Commander US Army Aviation Systems Command ATTN: AMSAV-ES 4300 Goodfellow Blvd St. Louis, MO 63120-1798
1	Director US Army Aviation Research & Technology Center Ames Research Center Moffett Field, CA 94035-1099
1	Commander US Army Communications - Electronics Command ATTN: AMSEL-ED Ft. Monmouth, NJ 07703-5301
1	Commander CECOM R&D Technical Library ATTN: AMSEL-IM-L, Reports Section B. 2700 Ft. Monmouth, NJ 07703-5000
1	Commander US Army Missile Command ATTN: AMSMI-R Redstone Arsenal, AL 35898
1	Commander Naval Surface Weapons Center ATTN: Mr. P.T. Adams, Code G-35 Dahlgren, VA 22448-5000

DISTRIBUTION LIST

No. of Copies	Organization
1	Director Ballistic Missile Defense Advanced Technology Center ATTN: BMDATC-M, Dr. D.B. Harmon Huntsville, AL 35807
2	Director DARPA ATTN: Dr. Harry Fair Dr. Peter Kemmey 1400 Wilson Blvd Arlington, VA 22209
1	Commander US Army Tank Automotive Command ATTN: AMSTA-TSL Warren, MI 48397-5000
1	Commandant US Army Infantry School ATTN: ATSH-CD-CSL-OR Ft. Benning, GA 31905-5400
1	Commander US Army Development & Employment Agency ATTN: MODE-ORO Ft. Lewis, WA 98433-5000
5	Commander SDIO ATTN: SDIO/KEW, BG M. O'Neil MAJ R. Lennard SDIO/IST Dr. J. Ionson Dr. L. Caveny Washington, DC 20301-7100
1	Director US Army Research Office ATTN: Dr. Mikael Ciftan Research Triangle Park, NC 27709-2211
1	Sandia National Laboratory ATTN: Dr. Maynard Cowan, Dept 1220 PO Box 5800 Albuquerque, NM 87185
2	Commander Naval Research Laboratory ATTN: Dr. I.M. Vitkovitsky, Code 4701 Mr. R. Ford, Code 4474 Washington, DC 20375
1	AFWL/SUL Kirtland AFB, NM 87117
5	Air Force Armament Laboratory ATTN: AFATL/DLDODL ATATL/DLYS, CPT J. Brown LT J. Martin Mr. Kenneth Cobb LT D. Jensen Dr. Timothy Aden Eglin AFB, FL 32542-5000
1	AFAPL/POOS-2 ATTN: Dr. Charles E. Oberly Wright-Pattersen AFB Dayton, OH 45433
1	Director Brookhaven National Laboratory ATTN: Dr. J.R. Powell, Bldg 129 Upton, NY 11973
1	Director Lawrence Livermore National Lab ATTN: Dr. R.S. Hawke, L-156 PO Box 808 Livermore, CA 94550
3	Director Los Alamos National Laboratory ATTN: MSG 787, Mr. Max Fowler Dr. Gerry V. Parker Dr. Mark Parsons, MS D472 Los Alamos, NM 87545
2	GA Technologies, Inc. ATTN: Dr. Robert Bourque Dr. L. Holland PO Box 85608 San Diego, CA 92138

DISTRIBUTION LIST

No. of Copies	Organization
1	NASA Lewis Research Center ATTN: Lynette Zana, MS 501-7 2100 Brook Park RD Cleveland, OH 44135
1	Astron Research & Engineering ATTN: Dr. Charles Powars 2028 Old Middlefield Way Mountain View, CA 94043
2	Austin Research Associates ATTN: Dr. Millard L. Sloan Dr. William E. Drummond 1091 Rutland Drive Austin, TX 87858
2	Maxwell Laboratories ATTN: Dr. Rolf Dethlefson Dr. Michael M. Holland 8888 Balboa Avenue San Diego, CA 92123
3	Electromagnetic Research, Inc. ATTN: Dr. Henry Kolm Dr. Peter Mongeau Mr. William Snow 625 Putnam Avenue Cambridge, MA 62139
1	BDM Corporation ATTN: Dr. David Elkin 10260 Old Columbia RD Columbia, MD 21046
1	Boeing Aerospace Company ATTN: Dr. J.E. Shrader PO Box 3999 Seattle, WA 98134
2	IAP Research, Inc. ATTN: Dr. John P. Barber Dr. David P. Bauer 2763 Culver Ave. Dayton, OH 45459-3723
1	LTV Aerospace & Defense Company ATTN: Dr. Michale M. Tower Dr. C.H. Haight,M/S TH-83 PO Box 65003 Dallas, TX 75265-0003
5	GT Devices ATTN: Dr. Derek Tidman Dr. Shyke Goldstein Dr. Neils Winsor Dr. Y.C. Thio Dr. Rodney L. Burton 5705-A General Washington Drive Alexandria, VA 22312
1	General Dynamics ATTN: Dr. Jaime Cuadros PO Box 2507 Pomona, CA 91766
1	General Electric Company ATTN: Dr. John Hickey, Bldg 37 Room 380 1 River RD Schnectady, NY 12345
3	General Electric Company (AEPD) ATTN: Dr. William Bird Dr. W. Condit Dr. Slade L. Carr RD#3, Plains RD Ballston Spa, NY 12020
1	General Research Corporation ATTN: Dr. William Isobell 5383 Hallister Avenue Santa Barbara, CA 93111
1	Gould Defense Systems, Inc. Ocean Systems Division ATTN: Dr. Donald M. McEligot One Corporate Place Newport Corporate Park Middletown, RI 02840
1	SAIC ATTN: Dr. Dan Barnes 206 Wild Basin RD, Suite 105 Austin, TX 78746
1	Systems Planning Corporation ATTN: Donald E. Shaw 1500 Wilson Blvd

DISTRIBUTION LIST

No. of Copies	Organization
1	Pacific-Sierra Research Corp. ATTN: Dr. Gene E. McClellan 1401 Wilson Blvd Arlington, VA 22209
3	Physics International Company ATTN: Dr. A.L. Brooks Dr. Edward B. Goldman Dr. Frank Davies 2700 Merced Street San Leandro, CA 94577
1	R&D Associates ATTN: Dr. Peter Turchi PO Box 9695 Marina del Rey, CA 90291
1	Rockwell International Rocketdyne Division ATTN: Dr. Earl Deder, MS HB14 6633 Canoga Avenue Canoga Park, CA 91304
2	SAIC ATTN: Dr. Jad H. Batteh Mr. G. Rolader 1519 Johnson Ferry RD, Suite 300 Marietta, GA 30062
2	SAIC Plasma Physics Division ATTN: Dr. John Connally 1710 Goodrich Drive, T4 McLean, VA 22102
1	Univerisyt of Alabama in Huntsville School of Science & Engineering ATTN: Dr. C.H. Chan Huntsville, AL 35899
1	University of Miami ATTN: Dr. Manuel A. Huerta Physics Department PO Box 248046 Coral Gables, FL 33124
1	Electromagnetic Applications, Inc. ATTN: Dr. Ronal W. Larson 12567 W. Cedar Drive, Suite 250 Lakewood, CO 80228-2091
1	Westinghouse Electric Corporation Marine Division ATTN: Dr. Dan Omry Dr. Ian R. McNab 401 E. Hendy Avenue Sunnyvale, CA 94088-3499
1	Westinghouse R&D Laboratory ATTN: Dr. Bruce Swanson 1310 Beulah RD Pittsburgh, PA 15233
2	Auburn University ATTN: Dr. Raymond F. Askew, Director, Leach Nuclear Science Center Dr. E.J. Clothiaux, Dept of Physics Alabama 36849-3501
1	Texas Technical University Department of EE/Computer Science ATTN: Dr. M. Kristiansen Lubbock, TX 79409-4439
1	Tuskegee Institute Department of Mechanical Engng ATTN: Dr. Pradosh Ray Alabama 36088
2	University of Texas Center for Electromechanics Balcones Research Center ATTN: Mr. William Weldon Mr. John Gully 10100 Burnet RD, Bldg 133 Austin, TX 78758
1	University of Tennessee Space Institute ATTN: Dr. Dennis Keefer Tullahoma, TN 37388-8897

DISTRIBUTION LIST

Aberdeen Proving Ground

Dir, USAMSAA
ATTN: AMXSY-D
AMXSY-MP, H. Cohen
Cdr, USATECOM
ATTN: AMSTE-SI-F
Cdr, AMCCOM
ATTN: SMCCR-RSP-A
SMCCR-MU
SMCCR-SPS-IL

USER EVALUATION SHEET/CHANGE OF ADDRESS

This Laboratory undertakes a continuing effort to improve the quality of the reports it publishes. Your comments/answers to the items/questions below will aid us in our efforts.

1. BRL Report Number_____ Date of Report_____

2. Date Report Received_____

3. Does this report satisfy a need? (Comment on purpose, related project, or other area of interest for which the report will be used.)_____

4. How specifically, is the report being used? (Information source, design data, procedure, source of ideas, etc.)_____

5. Has the information in this report led to any quantitative savings as far as man-hours or dollars saved, operating costs avoided or efficiencies achieved, etc? If so, please elaborate._____

6. General Comments. What do you think should be changed to improve future reports? (Indicate changes to organization, technical content, format, etc.)

_____

_____

_____

CURRENT ADDRESS

_____
Name

_____
Organization

_____
Address

_____
City, State, Zip

7. If indicating a Change of Address or Address Correction, please provide the New or Correct Address in Block 6 above and the Old or Incorrect address below.

OLD ADDRESS

_____
Name

_____
Organization

_____
Address

_____
City, State, Zip

(Remove this sheet, fold as indicated, staple or tape closed, and mail.)

FOLD HERE

Director
US Army Ballistic Research Laboratory
ATTN: DRXBR-OD-ST
Aberdeen Proving Ground, MD 21005-5066

NO POSTAGE
NECESSARY
IF MAILED
IN THE
UNITED STATES

OFFICIAL BUSINESS
PENALTY FOR PRIVATE USE, $300

BUSINESS REPLY MAIL
FIRST CLASS PERMIT NO 12062 WASHINGTON, DC
POSTAGE WILL BE PAID BY DEPARTMENT OF THE ARMY

Director
US Army Ballistic Research Laboratory
ATTN: DRXBR-OD-ST
Aberdeen Proving Ground, MD 21005-9989

FOLD HERE

END

DATE

FILMED

FEB.

1988